Received: 31 May 2017 | Revised: 17 February 2018 | Accepted: 26 March 2018
DOI: 10.1002/etep.2602

RESEARCH ARTICLE

WILEY

Hybrid islanding detection with optimum feature selection and minimum NDZ

Sheetal Chandak[1] | Manohar Mishra[2] | Pravat Kumar Rout[2]

[1] Electrical Engineering Department, Siksha 'O' Anusandhan University, Bhubaneswar 751030, India

[2] Electrical and Electronics Engineering Department, Siksha 'O' Anusandhan University, Bhubaneswar 751030, India

Correspondence
Sheetal Chandak, Electrical Engineering Department, Siksha 'O' Anusandhan University, Bhubaneswar 751030, India.
Email: sheetalchandak91@gmail.com

Summary

Integration of the distributed generators into a distribution system encounters various system issues, and out of those islanding detection is 1 of the major protection problems to focus on. Many detection schemes have been proposed in the recent past, which possess a nondetection zone (NDZ) and usually neglect to provide a justification for the selected detecting features among all possible measures. Sensitive feature selection and minimization of NDZ are the 2 major objectives of this study. This paper comprises of 2 operational modes of designed IEEE 13-bus test feeder (offline mode and online mode of operation). The offline mode of system operation focuses on selecting the optimal feature vectors using the proposed "modified multiobjective differential evolution algorithm" coupled with an extreme learning machine classifier. The modified multiobjective differential evolution algorithm-extreme learning machine is applied to find out 2 optimum feature vectors, one by considering accuracy and minimal features and another one by dependability with a single feature as its objective functions. The online mode concentrates on the proposed new hybrid islanding detection method comprised of both passive and active detection techniques. Passive technique implements a decision tree designed by using the obtained accuracy-based feature vector. Decision tree triggers the active method on suspecting the runtime instances as non-islanding events to reduce the NDZ. Active method uses the obtained dependability-based feature vector as an injecting parameter. The test results indicate the efficiency and accuracy of the proposed approach under different circumstances of power mismatch.

KEYWORDS

decision tree, distributed generator, extreme learning machine classifier, feature selection, hybrid method, islanding detection, multiobjective differential evolution algorithm, nondetection zone

List of Abbreviations: DG, Distribution generators; DT, Decision tree; ELM, Extreme learning machine; FS, Feature selection; FP, False positive; FN, False negative; HIDM, Hybrid islanding detection method; IDM, Islanding detection method; MMODEA, Modified multiobjective differential evolutionary algorithm; NDZ, Nondetection zone; PWM, Pulse Width Modulation; SFS, Sandia frequency shift; SF, Scaling factor; TP, True positive; TN, True negative

List of Symbols: Cr, Crossover rate; y, ELM output; $f(x)$, Fitness function; $X_{i,\ G}$, Generated target vector; L, Hidden layer; x, Input samples for ELM; H^{*}, Moore Penrose generalized pseudoinverse; $V_{i,\ G}$, Mutant vector; N, Number of samples; G, Number of generation; β, Output weight matrix; X_{LB}, Predefined lower bound; X_{UB}, Predefined upper bound; P, Population size; ω_i, Random initialized weight; b_i, Random initialized biases; j_{rand}, Random integer; $U_{i,\ G}$, Trial vector; T, Target matrix

1 | INTRODUCTION

Countries have achieved a more diversified energy mix with the growth in community ownerships, which have led to an evolution of microgrids.[1] Microgrids can be portrayed as small-scale, localized distributed generators (DGs) installed near the load, comprising of their own power resources, generation, and storage. DGs encompassing renewable energy sources include wind farms, photovoltaic farms, small-scale hydroplants, fuel cells, and microturbines. Integration of DGs with utility grid using the concept of microgrids comes with many challenges. One of the major technical issues related with the interconnection of DGs is power islanding.

According to the IEEE standard 1547-2003,[2] an island can be defined as a condition where DG isolates from the grid and independently meets the local utility loads. This creates safety problems and power quality issues for the utility, along with the inability to maintain the voltage and frequency within acceptable operational limits. Thus, it becomes an essential issue to detect the instance of islanding and protect the DG. The IEEE standard defines a time of 2 seconds for islanding detection from the time of occurrence.[3] To have a clear idea about the islanding phenomenon, it becomes essential to draw attention towards its 2 significant characteristics. The first characteristic is known as nondetection zone (NDZ) criterion. The decisive factor NDZ can be defined as the range of power difference between the DG and load where the islanding detection technique fails to detect the test conditions. The second characteristic relates to the load types that can be modelled as a parallel RLC circuit and located in the islanded network. RLC load circuits are basically used for islanding analysis as they form the worst situations for islanding detection by the relevant schemes. Detection schemes for islanding are generally not affected by the nonlinear loads or loads with constant power.[4,5]

Detection of an islanding condition can broadly be distinguished into 2 schemes: remote and local schemes. Remote schemes are communication-based channels constructed between the DGs and the utility. Implementation of this method is uneconomical because of expensive communication equipment. On the other hand, local schemes are further categorized as passive and active detection method. Passive detection method follows a philosophy of computing and comparing the associated system parameters with the preset threshold value to find the detection of islanding condition. However, the active detection method works on the concept of deliberately injecting external perturbation continuously into the system and that small variation builds a greater fluctuation in system parameters to detect the islanding situation faster.[6]

Passive detection techniques possess some major preferable advantages like faster detection, no power quality issues, less complexity in design, and cost. System parameters for passive techniques play an important role in the detection of an islanding condition. Voltage, current, power, frequency, harmonic distortion, and their corresponding rate of change are considered as some of the detecting parameters for passive techniques. Several passive methods have been proposed by the researchers in the recent past.[7-13] However, all the suggested approaches possess a significant NDZ, as it is difficult to choose an appropriate threshold for the monitored system parameters. On the other hand, active detection techniques can detect an islanding condition even in the case of zero power mismatches between load side demand and generation and have a very small NDZ. Researchers have proposed various active methods by injecting system parameters such as current, voltage phase angle, harmonic impedance measurement, negative sequence current, rate of change of frequency (ROCOF), and rate of change of sequence components of currents.[14-19] The methods use positive feedbacks in the control loops to speed up the parameter to violate the threshold, resulting a faster detection of an islanded condition. But, the active method possesses a demerit of injecting perturbation in the system, which results in a degradation of system power quality. In addition to that, this method has a reduced capability to detect an island when there are several DGs supplying power to the same island.

To overcome the flaws of passive and active detection techniques, several HIDMs have been proposed. As per the name assigned "hybrid," these islanding detection methods (IDMs) use 2 different principles based on active and passive techniques at a time with an objective to suppress the limitation of 1 technique by incorporating the advantages of the other. Here, secondary IDM executes when the primary IDM fails to detect the islanding condition successfully. Several HIDMs have been proposed by the researchers in the recent past.[20-26] IDM presented in Menon and Nehrir[20] uses the positive feedback as active method and voltage unbalance as passive methods. Yin et al[21] proposed an HIDM using rate of change of voltage and adaptive reactive power shift. Mahat et al[22] proposed an HIDM using rate of change of voltage and real power shift. The passive technique based on Q-f droop curve and active technique based on sandia frequency shift are adopted in Vahedi et al.[23] HIDM using ROCOF (passive) and sandia frequency shift technique (active) are presented by Vahedi et al.[24] Zhou et al proposed a HIDM based on decision tree (DT) and positive feedback for distributed generations in Zhou et al.[25] By combining SMS, ROCOF, and under/over frequency relay, a HIDM is proposed in Akhlaghi et al.[26] HIDM suppresses the disadvantages of the both the passive and active methods. Thus, implementing hybrid detection approach improves the performance capability and efficiency of the technique. It reduces the NDZ and power quality issues.

In this paper, a HIDM is approached along with a major focus on selection of the best feature to design an efficient method for islanding detection. This paper is analysed in 2 modes: offline and online mode of operation.

1.1 | Offline mode of operation

Several detection techniques analysed and explained in references27-31 based on multiple features do not elaborate the process of selecting the set of best features from the list of features extracted. Extraction of a large number of features in real-time environment increases the computational burden, and hence, the selection of minimum number of most appropriate features for detection becomes an important concern. Along with that, feature selection (FS) reduces the training time and computational time of a classifier for classification and improves the classification accuracy by eliminating the redundant features. Therefore, it is necessary to extrapolate a selection process for getting a universal detection feature set, which can secure all the DGs integrated with the utility.

This mode focuses on the selection of sensitive features that help in fast and accurate islanding detection. Hence, the FS method has been elaborated thoroughly in this paper. Three major steps required to prepare a robust islanding detection technique are feature extraction, selection, and classification. Emphasizing on the selection of optimal features for the IEEE 13-bus system, 16 features are extracted from the voltage and current signals at a sampling frequency of 3.8 kHz. Best set of feature is selected by performing modified multiobjective differential evolutionary algorithm (MMODEA) for all the DGs. Selected features are applied to an extreme learning machine classifier (ELM) classifier that can discriminate between islanded and nonislanded conditions.

1.2 | Online mode of operation

This mode focuses on implementing the sensitive features in the suggested detection technique for classification during the run time of the system. The proposed approach is a hybrid of passive IDM and active IDM. The passive method opted here is based on the obtained optimal feature vector using a decision tree method as a classifier for accurate detection. This method possesses a smaller detection time, higher accuracy and reliability, along with a smaller NDZ. To overcome the disadvantage of having a NDZ, passive method is coupled with an injection of disturbance into the system, if required. To resolve the power quality degradation issue, the active method is initiated for a short duration and is kept less than 3% of the feature variation. The proposed approach suppresses all the disadvantages of passive and active IDMs and functions efficiently with multiple DGs in a system.

Designing a detection method, using a well-justified set of feature is a major focus of this work. And thus, the major contribution of this paper can be pointed as:

1. Hybrid islanding detection scheme accompanied with a proposed FS technique (MMODEA).
2. Feature selections are carried out based on 2 main objectives such as accuracy with number of features and dependability with number of features.
3. Accuracy-based feature set used to design the passive method of HIDM.
4. Dependability-based feature set implemented in active method of HIDM.

Schematic representation of this paper is as follows: Section 2 covers detail about the designed system under study. Section 3 subsequently represents the different cases and features undertaken for this study. Section 4 highlights the idea of FS using multiobjective differential evolutionary algorithm followed by its analysis in Section 5. The proposed HIDM is discussed in Section 6. Further, the performance analysis of the considered HIDM is presented in Section 7. A detail discussion on the offline and online mode approach is presented in Section 8. At the end in Section 9, the concise summary of the work done and the measure finding concludes this paper.

2 | SYSTEM UNDER STUDY

The microgrid structure undertaken for this study is designed considering the ethical standards of IEEE 13-bus radial distribution test feeder[32] and extended with the DG integration. The schematic layout of 13-bus test feeder is represented in Figure 1A.

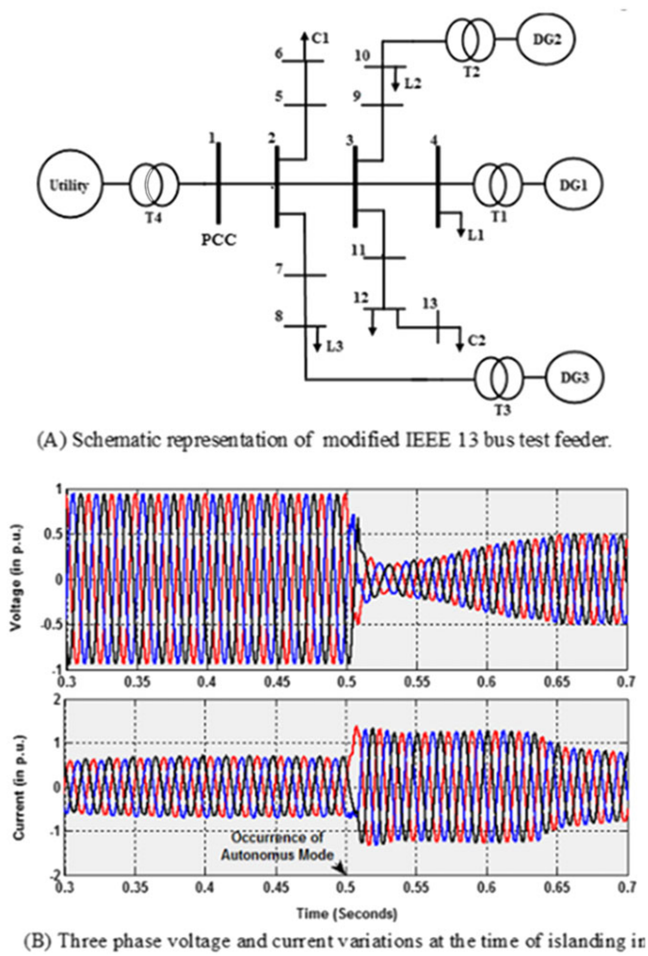

FIGURE 1 System studied and its response. A, Schematic representation of modified IEEE 13-bus test feeder. B, Three-phase voltage and current variations at the time of islanding in DG1

The 13-bus feeder is served by a substation transformer rating of 115/4.16 kV (delta/grounded wye). The feeder is lightly loaded uniformly and covers about 8200-ft length. There are 2 shunt capacitors at feeder ends, 1 of 200 kVAR in all the 3 phases at node 6 and another of 100 kVAR on 1 of the phases (C phase) at node 13. The operating parameters and model specifications are given in Table 1.

Expansion of feeder is done by integrating 3 types of DGs. The specification and rating of each DG are presented in Table 2. DG1 at node 4 is a wind turbine-driven doubly fed induction generator. The doubly fed induction generator is modelled by incorporating an induction generator and an IGBT-based pulse width modulation (PWM) converter. The stator winding is coupled directly with the utility.[33] However, the rotor winding is connected through an AC-DC-AC PWM. DG2 at node 10 is an inverter-based PV power generator coupled with a boost converter, and its MPPT technique is based on incremental and conductance (InC) method.[34] DG3 at node 8 represents a wind turbine type 4 power generating system. The type 4 wind turbine comprises of a synchronous generator linked with a diode rectifier, a DC-DC boost converter (IGBT based), and a DC-AC IGBT-based PWM converter.[35] The model is designed on the podium of MATLAB 2014/Simulink, and operation is based on IEEE 1547 Standards.

3 | CASES AND PARAMETERS FOR DATA GENERATION

For the purpose of differentiating between the islanding and non-islanding scenarios, ample numbers of practically assorted cases are performed so as to provide a firm dataset towards the application of MMODEA-ELM technique. Table 3 represents a detailed list of simulated cases used in this study.

TABLE 1 Model specifications

System Parameters	Specifications
Operating frequency	60 Hz
Quality factor	1
Transformer—T1	4.16 kV/575 V
Transformer—T2	4.16 kV/1750 V
Transformer—T3	4.16 kV/575 V
Transformer—T4	115 kV/4.16 kV
DG1 load—L1	1.5 MW, 0.652 MVAR
DG2 load—L2	0.9 MW, 0.435 MVAR
DG3 load—L3	2 MW, 0.87 MVAR
Shunt capacitor—C1	200 kVAR
Shunt capacitor—C2	100 kVAR

TABLE 2 DG specifications

Type of DGs	Rating
DG1	1.66 MVA (1.5/0.9 MVA)
DG2	1 MW
DG3	2.22 MVA (2/0.9 MVA)

TABLE 3 List of stimulated cases

Cases Studied	Case Type	Variations
Active power variation	Islanding	0%-±80%
Reactive power variation	Islanding	0%-±50%
Active and reactive power variation	Islanding	0%-±80%, 0%-±50%
Load switching	Non-islanding	Up to 20% overload
Capacitor switching	Non-islanding	0.5-10 MVAR
Fault scenarios	Non-islanding	Type LG, LL, LLG, LLL, LLLG Fault resistance varying from 0 to 100 Ω
Voltage sag	Non-islanding	0.1-0.9 p.u.
Voltage swell	Non-islanding	1.1-1.8 p.u.
DG tripping	Non-islanding	Tripping scheme: 1 DG, pair of DG At different load variations

3.1 | Islanding scenarios

To study the autonomous mode, several mismatch combinations of DG power generation and local load power consumption in the interior of the island are simulated. The power mismatch scenario ranges between perfect mismatch, small mismatch, and large mismatch on the basis of UL 1741 testing standards.[36] Active power mismatch extended between 0 and ±80%, whereas reactive power mismatch ranged from 0 to ±50%. The mismatch is so considered with an intention of overcoming the NDZ difficulty. Figure 1B shows the voltage and current variations at the time 0.5 second when the autonomous mode occurs. Cases are generated considering the RLC load as 1 of the worst case islanding scenarios. Events planned for generating the island as:

Case1 : *Small island*: This includes the DG and local load. The island can be formed at buses 4, 8, and 10 individually.

Case2 : *Medium island*: This comprises of local loads and multiple DGs when disconnected at bus 3 from the middle of the system model.

Case 3. : *Large island*: Taking into account all the DGs and loads of the system while getting disconnected from the main substation at bus 1.[30]

3.2 | Non-islanding scenarios

To facilitate the grid connected mode, 5 different cases of power system scenarios such as capacitor switching, load switching, line fault conditions, power quality events, and DG tripping are simulated as non-islanding events. The variations made with respect to all the above scenarios are enumerated in Table 3.

3.3 | Features studied

Multiple features are usually considered as a feature vector to secure islanding detection from any possible variations in the network. The most important reason of using different features is to allow the islanding detection technique with:

(a) Least NDZ at the DG location at reduced power mismatch.
(b) Application to multiple DG systems.
(c) Diversified operating conditions of the system.

In this work, all the combinations of system parameter indices focusing on multiple inverter-based DGs are measured. Along with that, every possible sensitive parameter of the system, the corresponding rate of change is also considered. Altogether, 16 possible features are measured, which can be actively affected by both islanding and non-islanding cases.[37] Features extracted in this study are mentioned in Table 4.

TABLE 4 List of features studied

Feature Notation	Feature Name (Magnitude in p.u.)	Symbolization of Feature
F-1	Rate of change of voltage w.r.t. time	dV/dt
F-2	Rate of change of frequency w.r.t. time	df/dt
F-3	Rate of change of active power w.r.t. time	dP/dt
F-4	Rate of change of reactive power w.r.t. time	dQ/dt
F-5	Rate of change of voltage w.r.t. frequency	dV/df
F-6	Rate of change of voltage w.r.t. active power	dV/dP
F-7	Rate of change of voltage w.r.t. reactive power	dV/dQ
F-8	Rate of change of frequency w.r.t. voltage	df/dV
F-9	Rate of change of frequency w.r.t. active power	df/dP
F-10	Rate of change of frequency w.r.t. reactive power	df/dQ
F-11	Rate of change of active power w.r.t. voltage	dP/dV
F-12	Rate of change of active power w.r.t. frequency	dP/df
F-13	Rate of change of active power w.r.t. reactive power	dP/dQ
F-14	Rate of change of reactive power w.r.t. voltage	dQ/dV
F-15	Rate of change of reactive power w.r.t. frequency	dQ/df
F-16	Rate of change of reactive power w.r.t. active power	dQ/dP

4 | PROPOSED FEATURE SELECTION APPROACH (OFFLINE MODE)

Features possess a complex relationship among each other which generates a demanding task of FS. Features individually may perform accurately for selection, but when performing together in the group may behave redundantly (or vice versa). Hence, the selection of an optimal feature subset which can properly distinguish between the classes having diversified properties becomes vital.

Depending on the evaluation criteria, FS algorithm can be broadly categorized into 2 types: filter approaches and wrapper approaches.[38] The major difference between these 2 is that the wrapper methods take the help of a classifier learning process while evaluating the feature subset and filter approaches do not. For the islanding detection problems, a filter approach named as backward and forward sequential FS is successfully implemented in Faqhruldin et al.[30] Faster execution is 1 of the main advantages of filter approach, whereas the selection of large subsets and lesser generality are few of the limitations affecting its performance. However, on the other hand, the wrapper approach attains better accuracy with lesser subsets and higher ability to generalize. In Samantaray et al and Kar and Samantaray,[28,31] the authors implemented decision tree and fuzzy logic classifiers for FS to detect islanding condition based on wrapper approach concept.

Selection of features itself is a challenging task, as the features themselves possess a complex relation with each other. Along with that, vast search space increases the selection complexity as it increases exponentially with the number of features present in the dataset.[39] Considering the above problem, a competent search technique is required. A population-based global optimization technique named as differential evolution (DE) technique was proposed by Storn and Price in the year 1997. DE is a simple, reliable, robust, and efficient global searching method. Because of the abovementioned advantages, DE is widely accepted by many researchers in different fields for FS. The detailed study on DE for FS is explained in Ali et al.[40]

To deal with an optimization problem, a single objective may not satisfactorily address the multiple aspects of a problem. Thus, a multiobjective optimization is favoured over a single objective optimization technique, particularly in the case of complex dataset. Considering the wrapper FS method, many classification techniques have been used by many researchers. Extreme learning method, a recent classifier algorithm, is a single feed forward network.[41] Being a recent technique, ELM is not extensively explored in the area of FS. However, ELM is known for its own advantages of possessing an attractive property of noniterative linear solution, which speed ups the magnitude to 5 times and 6 times as compared to multilayer perceptron and support vector machine respectively.[42] An ELM is used to improve the stability of the algorithm and to provide a robust unified solution. Apart from that, ELM does not need a parameter tuning and has less computational complexity. This paper present a MMODEA coupled with ELM classifier for multiple inverter-based DGs for islanding detection. The 3 basic objective functions are maximization of accuracy, maximization of dependability, and minimization of number of features for optimal FS. The proposed algorithm has been applied to the generated dataset of 2064 instances, and the results with selected set of features reveal the efficiency of the proposed model.

4.1 | Modified multiobjective differential evolution

4.1.1 | Basic differential evolution and its variant

Differential evolution being an optimization process helps in optimizing (maximize/minimize) problem w.r.t. a fitness function, ie, minimize $f(x)$/maximize $f(x)$.[43] It randomly initializes a target vector of P size population with D dimensional parameter vector. Generated target vector ($X_{i,\,G}$) can be represented as $X_{i,\,G} = \{X_{i,\,G,\,1}, X_{i,\,G,\,2} ... X_{i,\,G,\,D}\}$, where i varies from [1, P] and G represents the current generation. Each parameter of target vector is randomly initialized within a search space, restricted by predefined lower bounds, $X_{LB} = \left\{x_{LB}^1, x_{LB}^2 ..., x_{LB}^D\right\}$, and upper bounds, $X_{UB} = \left\{x_{UB}^1, x_{UB}^2 ..., x_{UB}^D\right\}$.

Then, a mutant vector $V_{i,\,G}$ of D dimension is generated using 1 of the mutation strategies *DE/rand/1* as stated in 1.

$$V_{i,G} = X_{r_1^i,G} + SF\left(X_{r_2^i,G} - X_{r_3^i,G}\right), r_1 \neq r_2 \neq r_3 \neq i \tag{1}$$

where r_1^i, r_2^i, r_3^i are randomly selected solutions from Gth generation and SF is a scaling factor varying from [0, 1].

By performing a crossover technique on the individual solutions of target vector and mutant vector using 2, a trial vector ($U_{i,\,G}$) is generated. The trial vector can be represented as $U_{i,G} = \left\{u_{i,G}^1, u_{i,G}^2 .... u_{i,G}^D\right\}$

$$u_{i,G}^{j} = \begin{cases} v_{i,G}^{j}, & if\left(\text{rand}_{j}[0,1) \leq Cr\right) or j = j_{rand} \\ x_{i,G}^{j}, & Otherwise \end{cases} \tag{2}$$

Here, $j = 1$, 2...D, Cr is the crossover rate that varies between [0, 1], and j_{rand} presents random integer within [1, D]. The fitness value of target vector and corresponding trial vector solutions are evaluated and compared using 3.

$$X_{i,G+1} = \begin{cases} U_{i,G}, & iff\left(U_{i,G}\right) \leq f\left(X_{i,G}\right) \\ X_{i,G}, & Otherwise \end{cases} \tag{3}$$

where i ranges from [1, P].

DE being an iterative process, mutation, crossover, and selection steps is repeated till the stopping criterion is reached.

4.1.2 | Multiobjective

Multiobjective optimization is a multicriteria decision making technique that involves more than 1 objective function to be optimized simultaneously. It involves minimization or maximization of multiple contradictory objective functions. Feature selection can be considered as a multiobjective optimization problem, where the main objective is to minimize the number of features and maximize the classification performance parameter. This can generate a Pareto front of nondominated feature subset to meet the requirements of objective function.[44]

Expressing in mathematical form, the optimization of multiple objective functions can be represented as expressed in 4.

$$optimize,\ F(x) = optimum\ \{f_1(x), f_2(x), ..f_n(x)\} \tag{4}$$

Here, x represents all possible set of features of a dataset, n presents the number of objective function selected for optimization, and optimum signifies either minimization or maximization depending on the objective functions. The set of nondominated Pareto optimal solutions forms a Pareto front, and the best solution can be extracted based on user's necessity.

4.1.3 | Modified multiobjective differential evolution

If the selection process of DE is closely analysed, it can be found that this step may miss out on some good solutions. Thus, the selection step implemented here is inspired by elitism-based nondominating sorting from NSGA-II.[45] Here, the solutions obtained from target vector and trial vectors (each of size P) are merged to form a population of size 2P. Each solution of the population of size 2P is ranked and sorted based on nondomination principle. Hence, the top best solutions of size P are selected for next-generation based on nondomination rank and crowding distance.[45] The proposed modified algorithm, MMODEA, operates for a number of independent iterations (NIter) to select the best feature subset on the basis of objective functions as presented in flow chart (Figure 2).

4.2 | Extreme learning machine

Extreme learning machine is a feed forward artificial neural network algorithm with a single hidden layer. It has gained huge attention among researchers because of its generality, learning speed, and consistency compared to other neural network techniques.[42] It has a salient feature of random selection of input weight and bias. It also facilitates the analytical determination of the output weight using *Moore Penrose generalized pseudoinverse*.[46] ELM intends to attain minimum training error as well as least norm of output weights. Thus, it provides the best results after overcoming the traditional issues like local minima, learning rate, training period, and stopping criterion. Structure of preliminary ELM is shown in Figure 3.

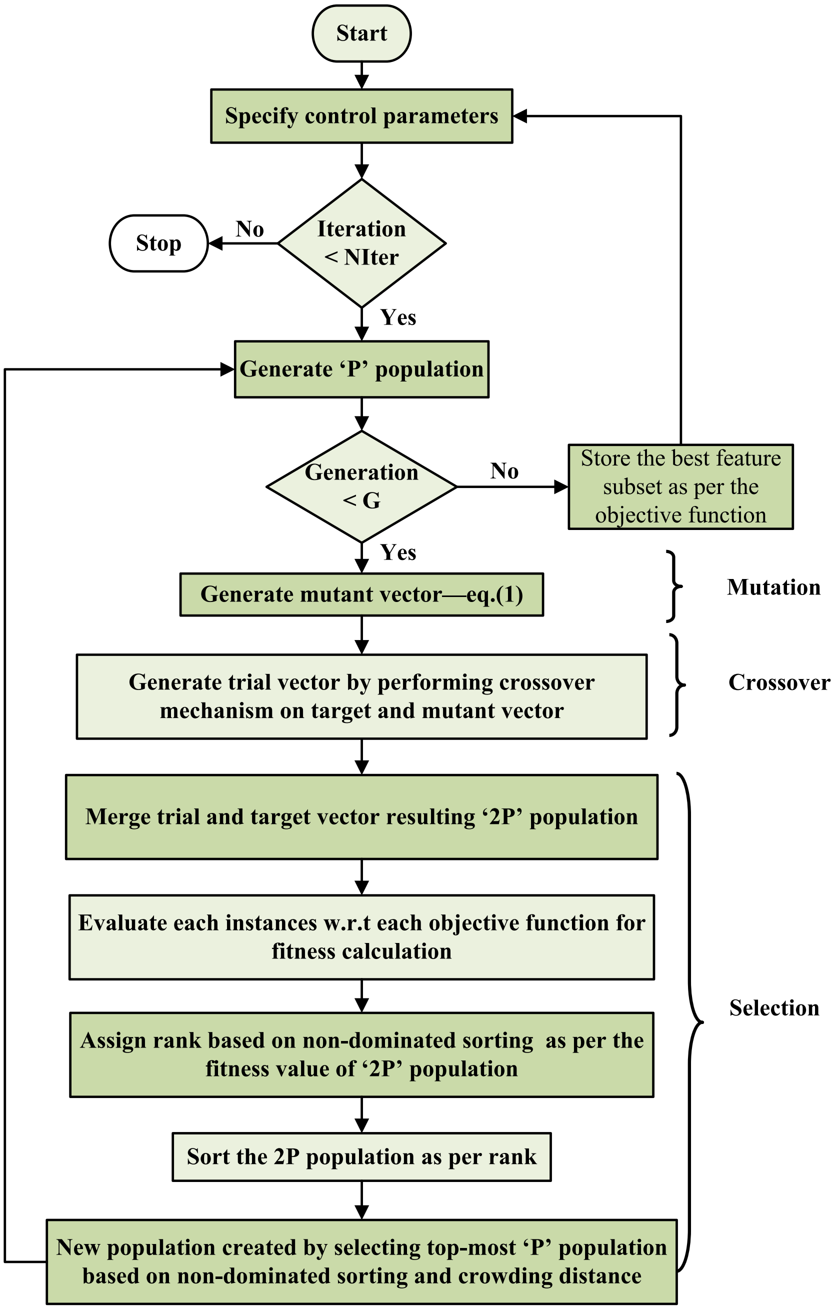

FIGURE 2 Algorithm for proposed MMODEA

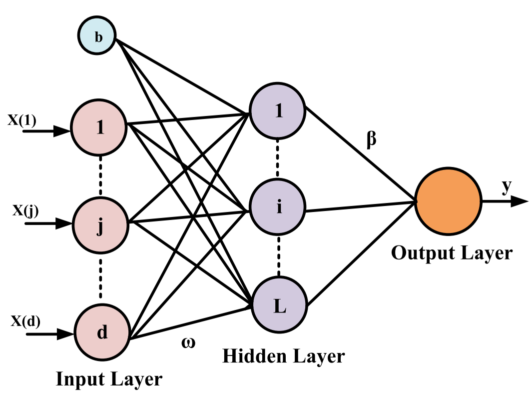

FIGURE 3 Preliminary ELM structure

ELM output (y) with the hidden nodes (L) is written in 5 as:

$$y = \sum_{i=1}^{L} \beta_i g_i(x) = \sum_{i=1}^{L} \beta_i G(\omega_i, b_i, x) = H\beta \tag{5}$$

Here, x denotes input samples; ω_i *and* b_i represents randomly initialized weights and biases respectively; $g_i(x) = G(\omega_i, b_i, x)$ corresponds to output function for ith hidden layer; H and β stands for the output matrix of hidden layer and weight respectively.[47] For N distinct samples (x_j, t_j), j $\in [1, N]$, the equation can be written as:

$$H\beta = T \tag{6}$$

where $H = \begin{bmatrix} h(x_1) \\ \vdots \\ h(x_N) \end{bmatrix} = \begin{bmatrix} G(\omega_1, b_1, x_1) & \cdots & G(\omega_L, b_L, x_N) \\ \vdots & \vdots & \vdots \\ G(\omega_1, b_1, x_N) & \cdots & G(\omega_L, b_L, x_N) \end{bmatrix}_{N\times L}$, $\beta = \begin{bmatrix} \beta_1 \\ \vdots \\ \beta_N \end{bmatrix}_{L\times 1}$, $T = \begin{bmatrix} T_1 \\ \vdots \\ T_N \end{bmatrix}_{N\times 1}$ and T is the target matrix.

The only parameter to be evaluated in ELM is the output weight matrix β, which is calculated using least squares estimation.

$$\beta = H^* T \tag{7}$$

Here, $H^* = (H^T H)^{-1} H^T$ known as Moore Penrose generalized pseudoinverse of the matrix H. ELM follows simple procedures of 3 steps as:

1. Random generation of hidden parameter.
2. Evaluation of matrix H for hidden layer.
3. Evaluation of output weight β using 7.

The whole process for evaluating P can be completed with a single iteration; this makes the ELM significantly fast.

4.3 | Objective function formulation

The selection of the best features is done by considering the number of features and their performance results based on the 2 objective functions. The performance parameters considered as objective functions in this study are dependability, accuracy, and number of feature. They are evaluated from TP, TN, FP, and FN:

$$\text{a) } Dependability{:}D = \frac{Predicted\ number\ of\ islanding\ cases}{Summation\ of\ actual\ islanding\ cases} = \frac{TP}{TP + FN} \tag{8}$$

$$\text{b) } Accuracy{:}A = \frac{Summation\ of\ correct\ prediction}{Summation\ of\ total\ number\ of\ actual\ cases} = \frac{TP + TN}{TP + FP + TN + FN} \tag{9}$$

Here, TP, TN, FP, and FN represents true positive, true negative, false positive, and false negative respectively. TP and TN provide correct prediction for islanding and non-islanding cases respectively. Whereas, FN and FP give a wrong prediction of islanding cases as non-islanding cases and vice versa respectively.

In the abovementioned analysis, dependability as represents in 8 states the correct prediction of islanded cases from the total number of islanding cases. Dependability as an objective function reduces the rate of misleading. Accuracy is considered as an important function because it measures the correct case prediction for both islanded and nonislanded scenarios as shown in 9.

5 | ANALYSIS OF FEATURE SELECTION APPROACH

Considering almost every scenario of frequently occurring fault conditions in microgrid environment, the designed model is studied and a close observation of variation of system parameters is done. The main objective of this work is to design a HIDM, comprising of passive and active detection approach. To obtain a justified feature set for designing a passive approach, MMODEA is implemented using 2 objective functions, such as accuracy and minimum number of features. Similarly, to obtain a highly justified sensitive feature as an injecting parameter, MMODEA is again operated using 2 objective functions: highest dependability with only 1 number of feature. Thus, the 2 differently obtained feature sets are used to design the proposed approach. To extract the best possible feature set on the basis of objective function independently, a total data set of 900 islanding cases and 1164 non-islanding cases are tested in proposed FS algorithm (MMODEA-ELM). Table 5 shows the sample of output results, representing the best feature sets for islanding and non-islanding event classification based on dependability and accuracy individually.

The optimal feature set obtained on the basis of accuracy is used as passive parameter to study the variations, whereas the feature subset obtained while considering the maximization of dependability as an objective function is used as an active injection feature in the proposed HIDM. The obtained results clearly indicate that the feature vector may contain 2 or more number of features so as to optimally justify the objective functions. However, to reduce the computational burden during the feature extraction stage, the feature vector must be chosen, including minimum number of features. Moreover, the selected feature set should ensure better performance in extremely noisy environments.

Therefore, the obtained feature sets are further cross-validated using ELM classifier at different noisy environments (with SNR equal to 20 and 30 dB), and the corresponding results are depicted in Table 6. Results illustrate that the feature sets perform efficiently in 30 dB noisy environment, having dependability and accuracy more than 90%. However, at 20 dB noise, the performance of objective functions decreases comparatively. On comparing all the obtained feature subset based on the performance of objective function at 20 dB, the most effective feature set is found to be [F9] having dependability *as* **94.77%** and a feature set [F1 F2 F4] having accuracy as **96.68%**.

To justify the results obtained from the above analysis, all the features from the selected feature vector are studied during the online mode of the test system.

6 | PROPOSED HIDM (ONLINE MODE)

Feature sets selected on the basis of dependability and accuracy are used in designing the proposed HIDM. The approach comprises of a passive detection and an active detection technique. The passive method is formed using the preferred feature set with higher accuracy. Accuracy as an objective function gives the percentage of correct prediction for both islanded and nonislanded case. Thus, a decision tree is planned using the features [F1 F2 F4] obtained from the selected accuracy-based feature vector. Passive method in the proposed approach gives an accuracy of 94.24%, which leaves behind a NDZ as shown in Table 7. To reduce the NDZ to 0%, an active method is coupled with the passive detection method. The active method addresses an injection of disturbance into the system so as to speed up the feature threshold violation while being disconnected from the grid. The disturbance injecting feature is opted according to the dependability-based feature set. Dependability gives a correct prediction of islanding cases from the total number of islanding cases. So, the feature [F9] having higher dependability is selected for injection into the system. Moreover,

TABLE 5 Performance of proposed algorithm for feature selection based on dependability and accuracy

Features	Dependability
[F2]	100%
[F8]	100%
[F9]	100%
[F15]	100%
Features	**Accuracy**
[F1 F2]	100%
[F1 F2 F4]	100%
[F6 F8 F15]	100%
[F1 F2 F8 F15]	100%

TABLE 6 Performance of ELM classifier on selected feature vectors

At 30 dB Noisy Conditions	
Features	**Dependability**
[F2]	96.07%
[F8]	95.42%
[F9]	100%
[F15]	96.07%
Features	**Accuracy**
[F1 F2]	98.70%
[F1 F2 F4]	98.88%
[F6 F8 F15]	97.54%
[F1 F2 F8 F15]	97.83%
At 20 dB Noisy Conditions	
Features	**Dependability**
[F2]	92.81%
[F8]	90.84%
[F9]	**94.77%**
[F15]	91.50%
Features	**Accuracy**
[F1 F2]	95.52
[F1 F2 F4]	**96.68%**
[F6 F8 F15]	94.37%
[F1 F2 F8 F15]	94.66%

TABLE 7 Accuracy performance of DT for different power mismatch

Power Mismatch During Islanding Scenarios	**Detection Accuracy**
±80% to ±60% active power variation	100%
±60% to ±40% active power variation	100%
±40% to ±20% active power variation	100%
±20% to ±10% active power variation	98.60%
±10% to 0% active power variation	78.48%
±50% to ±30% reactive power variation	100%
±30% to ±10% reactive power variation	99.25%
±10% to 0% reactive power variation	77.58%
Overall	94.24%

for less sensitivity to the sudden change in load, feature [F9] gives higher responsiveness as the grid is absent to retain the variations. Schematic representation of the proposed approach is represented in Figure 4.

The proposed approach is tested during the run time of the designed IEEE 13-bus test feeder. While the test system is operating, basic system parameters (ie, voltage, current, and frequency) are measured. These basic parameters are instantly used to calculate the selected features F1, F2, and F4 representing dv/dt, df/dt, and dq/dt respectively. This measurement and calculation of features is continuously observed with the run time of the system. On perceiving

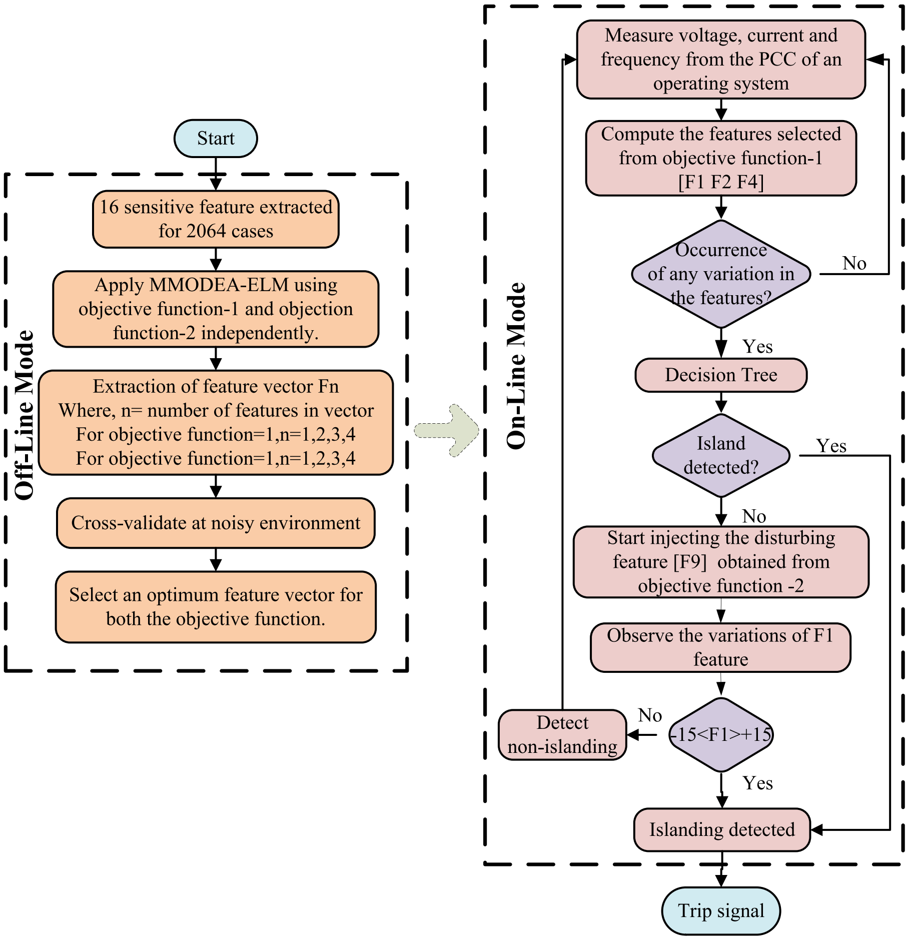

FIGURE 4 Flow chart of the proposed offline and online approach

any variation in the selected features, the decision tree is triggered for the next 5 cycles to study the type of disturbance occurred in the system. The decision tree is planned such that it can easily differentiate the islanding and non-islanding conditions. Figure 5 presents the schematic layout of the decision tree using the features F1, F2, and F4 with their corresponding threshold values. The threshold setting is carried out in this study by repeated analysis of islanding and non-islanding events.

If the case tested in decision tree concludes to be an islanding event, then an immediate trip signal is triggered, else the case is further validated through the proposed active method by injecting feature F9 as perturbation in the system for another 5 cycles. The disturbance injected into the inverter-based DG via a constant P-Q-based controller illustrated in Figure 6.

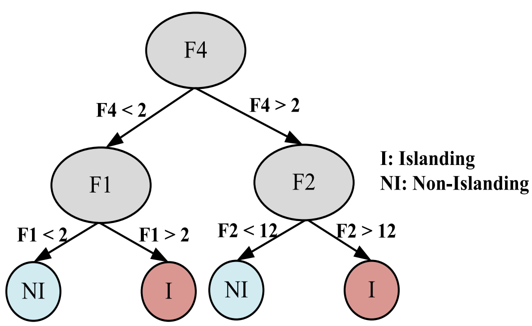

FIGURE 5 Decision tree

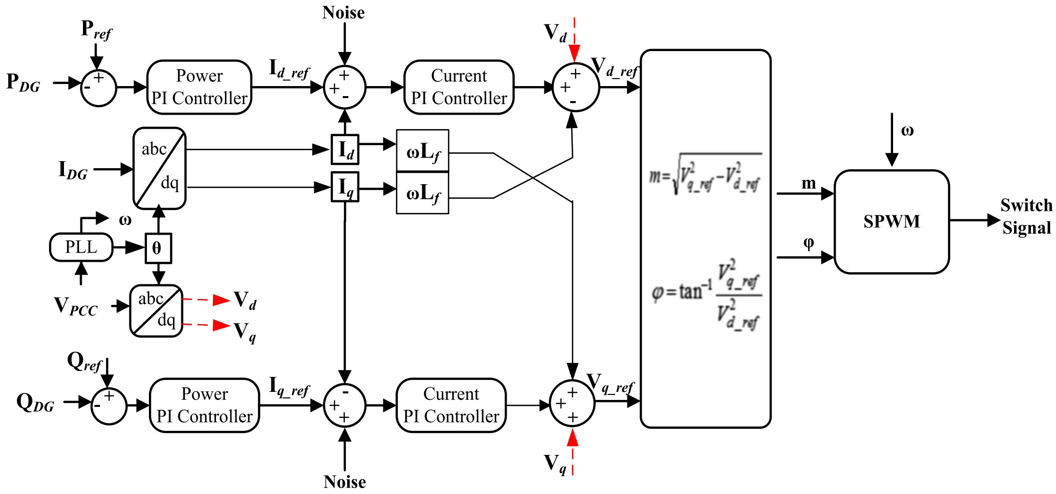

FIGURE 6 Interface control strategy for each DG

When the disturbance injection is triggered, feature F1 is observed. If feature F1 violates the second predefined limit within ±15 p.u., then the missed out islanding event is detected with a trip signal. This approach reduces the NDZ to 0% as the islanding events with smaller mismatches are easily detected.

7 | ANALYSIS OF PROPOSED HIDM

In real-time measurements, the voltage, current, and frequency are measured from the point of common coupling of microgrid and the corresponding DG ends. The basic measurements are evaluated to obtain the values of the predictor vector set [F1 F2 F4]. These values obtained for 5 cycles during the run time are compared with the predefined threshold values based on which the classification model of DT is planned and necessary control actions are implemented.

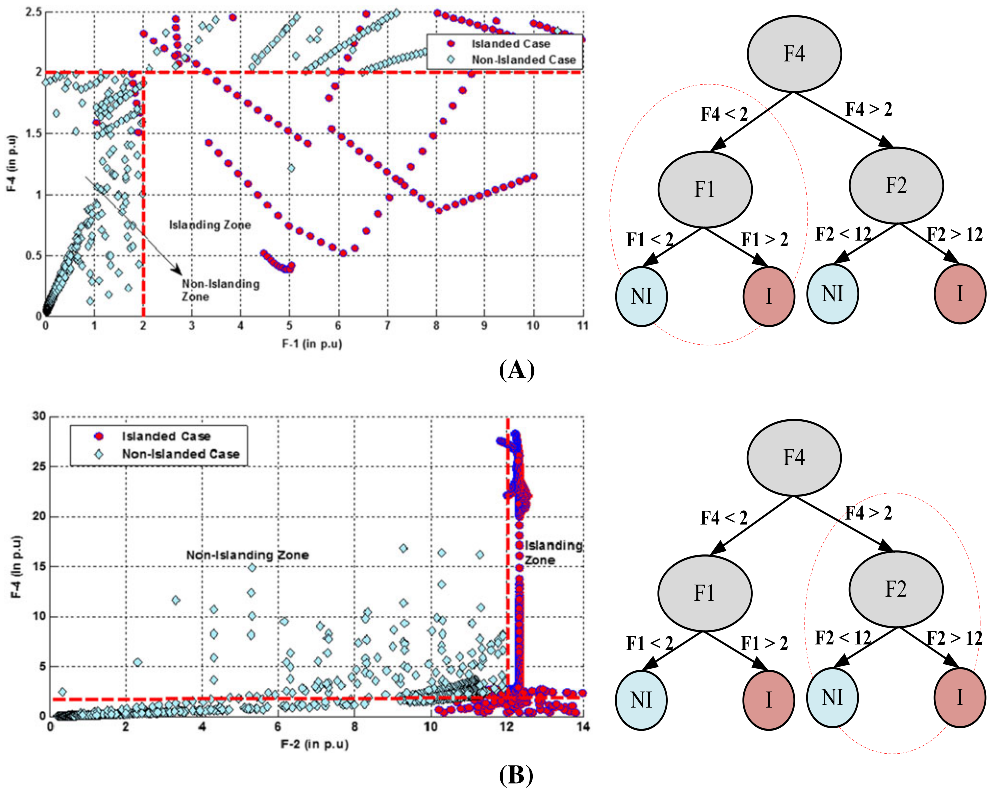

FIGURE 7 Scatter plot analysis to design a DT for setting threshold values: A, F1 versus F4 and B, F2 versus F4

7.1 | Performance analysis of decision tree

An overall analysis to design a DT through scatter plot for all the instances is pictographically presented in Figure 7. On observing Figure 7A, it is clearly visualized that maximum number of non-islanding cases is clustered within 0 to 2 p.u. range of feature F4 (taken in *y*-axis). And feature F1 (taken in *x*-axis) shows a clear distinction between islanding and non-islanding events at *x*-axis = 2 p.u. However, the set point of 2 p.u. can be extended but will result in false detection of an islanding event as non-islanding and vice versa. Thus, the threshold value to detect an islanding and non-islanding event can be defined as (F4 < 2 p.u. and F1 > 2 p.u.) and (F4 < 2 p.u. and F1 < 2 p.u.) respectively. Further analysing Figure 7B, for F4 > 2 p.u., the islanding and non-islanding events can easily be discriminated by feature F2 (taken in *x*-axis) at an approximate value of 12 p.u. The set point of 12 p.u. can be reduced but will result in false detection of many non-islanding event as islanding. Thus, the value is considered such that it covers maximum and minimum threshold

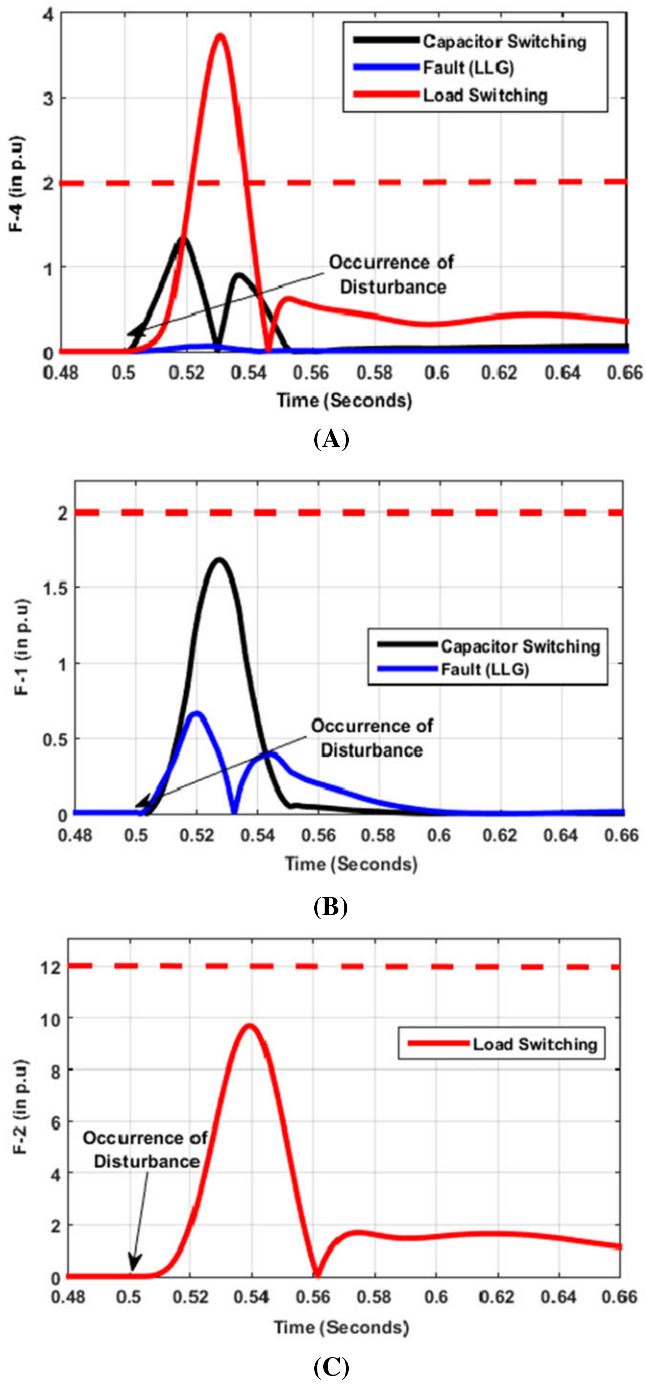

FIGURE 8 Case study on non-islanding event: A, variation in feature F4, B, variation in feature F1, and C, variation in feature F2

attained by non-islanding event and islanding event respectively. Consequently, the non-islanding zone and islanding zones are created using the threshold value set to design the DT as presented in Figure 5.

The sensitivity of the features used in forming a decision tree is analysed in a graphical form from Figures 8 to 11 for different system variation. In these figures, the dotted straight lines indicate the threshold setting values undertaken for this proposed approach.

7.1.1 | Case 1 features' response for non-islanding events

On analyzing Figure 8, it can be observed that feature F4 having a threshold value of 2 p.u. is crossed by load switching instance, while fault and capacitor switching instances remain within the range of less than 2 p.u. Thus, according to

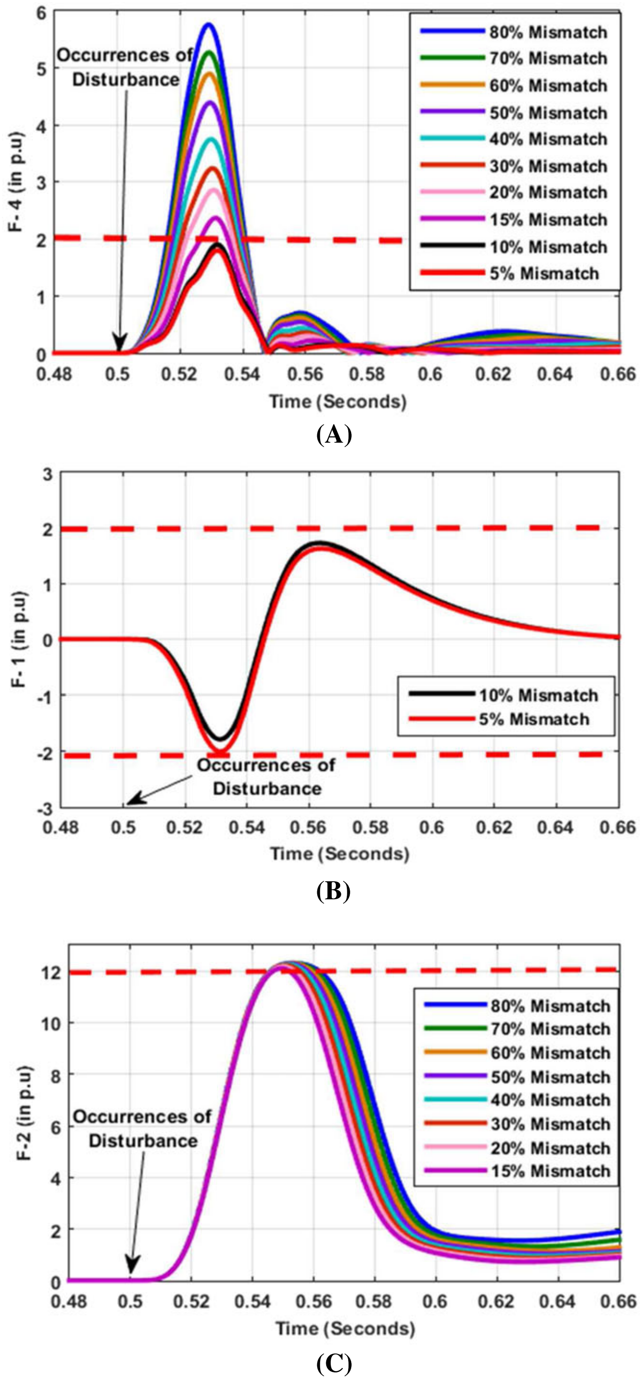

FIGURE 9 Analysis of islanding events with active power load mismatch: A, variation in feature F4, B, variation in feature F1, and C, variation in feature F2

the designed DT, load switching instance is further analysed by feature F2 as shown in Figure 8C, whereas fault and capacitor switching instances are forwarded towards feature F1 for classification and as presented in Figure 8B. On analyzing F1 and F2, all the instances are observed to be within the predefined threshold of ±2 and +12 p.u. respectively and hence conclude to be non-islanding instances.

7.1.2 | Case 2 features′ response for islanding events: P variations

Figure 9 illustrates the active power load mismatch variations for feature F4, F1, and F2 during islanding. On studying the variations, it is clear that from 15% to 80%, active power load mismatch events lie in a range greater than the set value (ie, = 2 p.u.) and the rest of the lower active power mismatch events lie in the lower range of set value. So, the

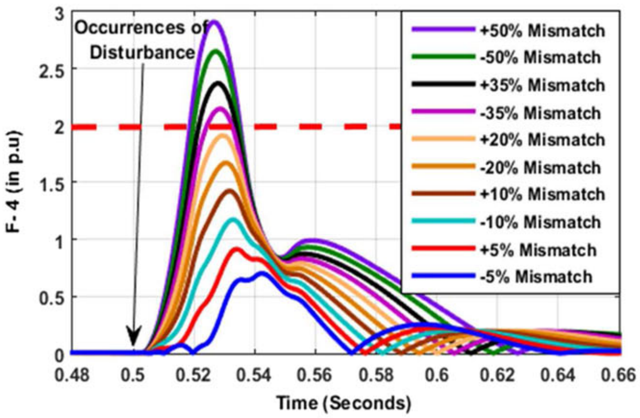

(A)

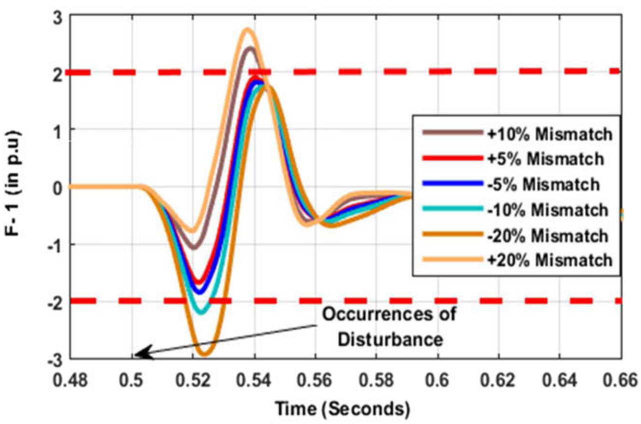

(B)

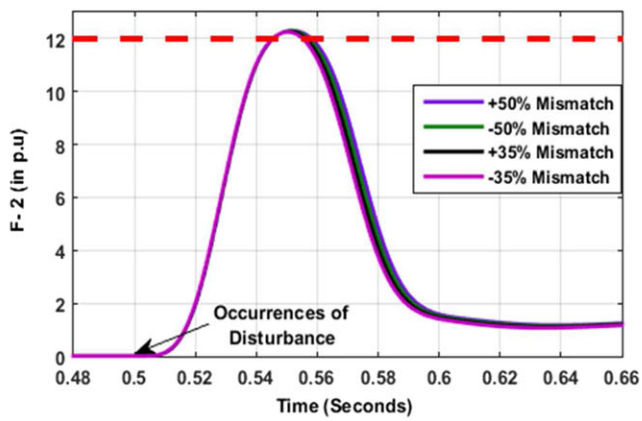

(C)

FIGURE 10 Analysis of islanding events with reactive power load mismatch: A, variation in feature F4, B, variation in feature F1, and C, variation in feature F2 events with below 10% of active power load mismatch are examined by the F1 node of the DT and the rest by the F2 node of DT. It can be observed from Figure 9B that events with below 10% of active power mismatch do not satisfy the threshold values set in DT for islanding detection and remains in the NDZ of DT. Whereas, the events examined at node F2 cross the set threshold value (ie, 12 p.u.) and are easily detected as islanding event within 3 cycles as observed from Figure 9C.

7.1.3 | Case 3 features′ response for islanding events: Q variations

The behavioural changes of features F4, F1, and F2 are presented in Figure 10, while studying the instances of reactive power mismatch during islanding. Figure 10A shows that all the instances between ±20% of reactive power load mismatch do not cross the set threshold, thus are further examined by feature F1. On examining feature F1 in Figure 10 B, it can be concluded that a small range of ±5% of reactive power load mismatch goes undetected and remains in the NDZ of DT. While other instances crossing the threshold of F4 are examined by feature F2 and on satisfying the threshold of F2, all the instances are detected perfectly as islanding in 2.5 cycles as shown in Figure 10C.

7.1.4 | Case 4 features′ response for islanding events: PQ variations

The system performance for active and reactive power load mismatch during islanding is shown in Figure 11. On analyzing the feature F4 variations, it can be observed that all the events cross the specific threshold of the feature and thus are verified at node F2. Every instance of power imbalance satisfies the threshold setting defined within 2.5 cycles from the occurrence of an islanding condition.

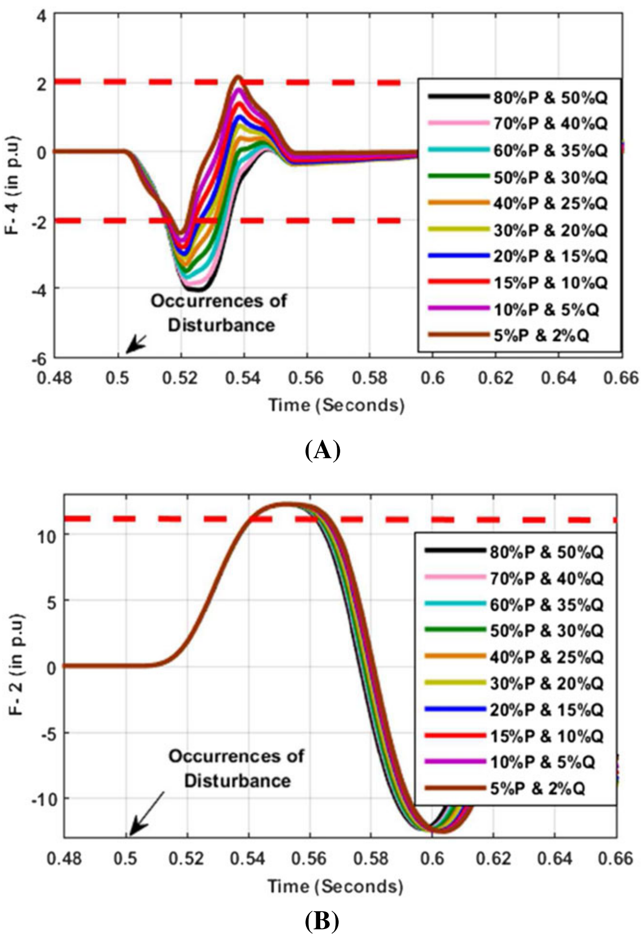

FIGURE 11 Analysis of islanding events with active and reactive power load mismatch: A, variation in feature F4 and B, variation in feature F2

Moreover, in Figure 7, the scatter plot of events implemented in DT also clearly illustrates that some instances of islanding case lie within the non-islanding zone, thus showing a presence of NDZ in proposed DT. To reduce the NDZ to zero, the DT approach is followed by an active method. A detailed analysis on the introduced active method is presented in the subsequent section.

7.2 | Performance response of active method

In active method, the selected dependability-based feature is used for injection. The injected value is set less than 3% of feature variations. The inception of disturbance injection occurs, if the DT fails to detect the event as islanding within its 5 cycles. As stated in Figure 4, the interruption is injected for a period of 5 cycles (ie, from 0.58 seconds to 0.66 seconds). The effect of injecting parameter on feature F1 is further examined to discriminate the undetected instances into islanding and non-islanding events. The second threshold specified for feature F1 in active method is ±15 p.u.

For islanding instances, the injection enhances the deviation to cross the threshold limit, but for non-islanding cases, the injection does not deviate the feature such that it crosses the threshold limit and remains nondetected. As observed before, some instances lie under the NDZ of DT. Verification of those instances with active method is shown in Figure 12. Showcasing a particular active power mismatch, it is observed that after injection at 0.58 seconds, the islanding events with smaller power mismatch are detected at 0.62 seconds as shown in Figure 12A. So for instances, which goes undetected as islanding gets detected after injection within 7.5 cycles from the occurrence of islanding. Whereas Figure 12B shows a non-islanding case which lies between the threshold limit of ±15 p.u. and is detected as non-islanding.

8 | DISCUSSION

Islanding protection is analysed by proposing offline and online mode of system operation. In offline mode, the proposed MMODEA yields out a feature vector [F1, F2, F4] and [F9] for accuracy and dependability respectively as

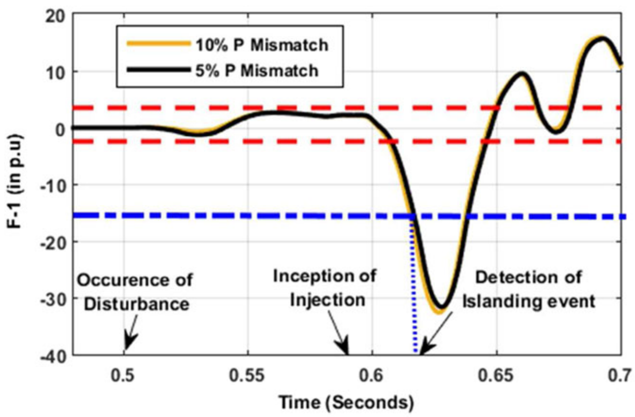

(A)

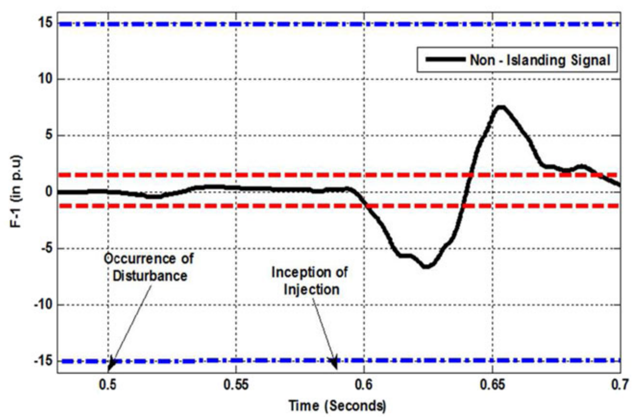

(B)

FIGURE 12 Feature F1 response for active approach: A, islanding event and B, non-islanding event

TABLE 8 Accuracy performance of active approach for smaller power mismatch

Power Mismatch During Islanding Scenarios	Detection Accuracy
±10% to 0% active power variation	100%
±5% to 0% reactive power variation	100%

TABLE 9 Comparison of the proposed method with the existing methods

Ref.	DG Type	Whether Feature Selection Used?	No. of Features Extracted	No. of Features Considered for Islanding Detection	Detection Time (Cycles)	Accuracy
El-Arroudi et al27	MS	No	11	11	-	91.6%
Samantaray et al28	MS	Yes (using DT)	11	3	-	100%
Faqhruldin et al29	MI	No	21	21	-	95.0%
Faqhruldin et al30	MS and MI	Yes (using forward and backward sequential FS)	21	4	11	100%
Kar and Samantaray31	MS and MI	Yes (using DT)	27	11	2	97.5%
Proposed approach	MS and MI	Yes (using MMODEA)	16	3	7.5	100%

MS, multiple synchronous DG; MI, multiple inverter-based DG; DT, decision tree.

objective function. Implementing the selected features set in online mode, the proposed HIDM functions on sensing the variations in the features. The passive detection method of HIDM is a DT classifier using feature F1, F2, and F4. In this work, the overall detection accuracy of the proposed DT is calculated as 94.24%, which leaves behind a NDZ of 5.76% as shown in Table 7. Islanding event is detected within 3 cycles by the DT classifier. DT is designed such that it gives faster decision and completely avoids the malfunctioning of relay. It is clearly observed that the detection accuracy is found to be 100% for the power mismatch (both active and reactive power) greater than ±20%. Moreover, it can be analysed that the detection accuracy gradually reduces, and is found to be only 77.58% and 78.48% for smaller reactive and active power mismatch (ie, 0% to ±10%) respectively. Therefore, this area of power mismatch (0% to ±10%) can be stated as NDZ of the designed DT-based passive approach. To eliminate this NDZ, the simulated cases are tested by the proposed active method as mentioned in the section. Active method implemented using feature [F9] increases the sensitivity, and deviations in the analysed feature reduce the NDZ to zero. The performance accuracy of active method is presented in Table 8, showing a NDZ of 0%. It takes a run-on time of 7.5 cycles (5 cycles for DT classification and +2.5 cycles after the injection of disturbance) to detect the instances lying within NDZ of DT.

Furthermore, to justify the application of proposed FS algorithm, for islanding detection, a comparative analysis has been done with respect to the number of features used as detecting parameters. Extracting a large number of features in real-time environment increases the computational burden, and hence, the selection of minimum number of most appropriate features for detection becomes an important concern. Along with that, FS reduces the training time and computational time of a classifier for classification and improves the classification accuracy by eliminating the redundant features. Therefore, Table 9 describes the superiority of the proposed method in comparison with the other existing approaches on the basis of type of DGs considered, application of FS, number of features extracted and studied, detection time taken, and accuracy.

9 | CONCLUSION

The proposed approach suggests 2 modes of operations implemented on modified IEEE 13-bus test feeder with multiple inverter-based DGs. In offline mode of operation, to select the optimum feature set, a novel FS approach based on MMODEA-ELM is proposed. The objective functions are formulated based on accuracy, dependability, and number of features to compute 2 optimum feature sets for better accuracy and dependability respectively. The proposed approach is cross-validated under various islanding and non-islanding conditions, even under 20 and 30 dB noisy environment. In online mode of operation, a HIDM is proposed comprising of a passive and an active detection method using the selected feature vectors. A DT-based passive method is designed by considering the obtained feature vector of better accuracy to detect islanding events. To further reduce the small NDZ present under different power mismatch conditions, an active method is triggered based on the obtained feature with better dependability for the non-islanding events detected from DT approach. For the cases under study, the suggested technique is capable of detecting islanding events in less than 7.5 cycles with an accuracy of 100% justifying its real-time application.

ORCID

Sheetal Chandak http://orcid.org/0000-0002-7751-4195
Manohar Mishra http://orcid.org/0000-0003-2160-4703

REFERENCES

1. World Energy Council, 'World Energy Resources Report', 2016.
2. IEEE Application Guide for IEEE Std 1547™: 'IEEE Standard for Interconnecting Distributed Resources with Electric Power Systems', 2009.
3. Lidula NW, Rajapakse AD. A pattern recognition approach for detecting power islands using transient signals—part I: Design and implementation. *IEEE Transactions on Power Delivery*. 2010;25(4):3070-3077.
4. Llaria A, Curea O, Jiménez J, Camblong H. Survey on microgrids: Unplanned islanding and related inverter control techniques. *Renew Energy*. 2011;36(8):2052-2061.
5. Samet H, Hashemi F, Ghanbari T. Minimum non detection zone for islanding detection using an optimal artificial neural network algorithm based on PSO. *Renew Sustain Energy Rev*. 2015 Dec 31;52:1-8.
6. Li C, Cao C, Cao Y, Kuang Y, Zeng L, Fang B. A review of islanding detection methods for microgrid. *Renew Sustain Energy Rev*. 2014;35:211-220.
7. Zeineldin HH, Kirtley Jr JL. Performance of the OVP/UVP and OFP/UFP method with voltage and frequency dependent loads. *IEEE Transactions on Power Delivery*. 2009;24(2):772-778.
8. De Mango F, Liserre M, Dell'Aquila A, Pigazo A. Overview of anti-islanding algorithms for PV systems. Part I: Passive methods. In power electronics and motion control conference, 2006. EPE-PEMC 2006. 12th international 2006 Aug 30 (pp. 1878-1883). IEEE.
9. Samet H, Hashemi F, Ghanbari T. Islanding detection method for inverter-based distributed generation with negligible non-detection zone using energy of rate of change of voltage phase angle. *IET Generation, Transmission & Distribution*. 2015;9(15):2337-2350.
10. Vatani M, Sanjari MJ, Gharehpetian GB. Islanding detection in multiple-DG microgrid by utility side current measurement. *International Transactions on Electrical Energy Systems*. 2015;25(9):1905-1922.
11. Freitas W, Huang Z, Xu W. A practical method for assessing the effectiveness of vector surge relays for distributed generation applications. *IEEE Transactions on Power Delivery*. 2005;20(1):57-63.
12. Hung GK, Chang CC, Chen CL. Automatic phase-shift method for islanding detection of grid-connected photovoltaic inverters. *IEEE Transactions on Energy Conversion*. 2003;18(1):169-173.
13. Merino J, Mendoza-Araya P, Venkataramanan G, Baysal M. Islanding detection in microgrids using harmonic signatures. *IEEE Transactions on Power Delivery*. 2015;30(5):2102-2109.
14. Hernandez-Gonzalez G, Iravani R. Current injection for active islanding detection of electronically-interfaced distributed resources. *IEEE Transactions on Power Delivery*. 2006;21(3):1698-1705.
15. Pourbabak H, Kazemi A. A new technique for islanding detection using voltage phase angle of inverter-based DGs. *International Journal of Electrical Power & Energy Systems*. 2014 May 31;57:198-205.
16. Zhu K, Wang Y, Lu X, Vieira J. A new DG anti-islanding protection technique based on harmonic impedance measurement. *International Transactions on Electrical Energy Systems*. 2016 Jan;1.
17. Gupta P, Bhatia RS, Jain DK. Active ROCOF relay for islanding detection. *IEEE Transactions on Power Delivery*. 2017;32(1):420-429.
18. Hamzeh M, Rashidirad N, Sheshyekani K, Afjei E. A new islanding detection scheme for multiple inverter-based DG systems. *IEEE Transactions on Energy Conversion*. 2016;31(3):1002-1011.
19. De Mango F, Liserre M, Dell'Aquila A. Overview of anti-islanding algorithms for pv systems. Part ii: Active methods. In power electronics and motion control conference, 2006. EPE-PEMC 2006. 12th international 2006 Aug 30 (pp. 1884-1889). IEEE.
20. Menon V, Nehrir MH. A hybrid islanding detection technique using voltage unbalance and frequency set point. *IEEE Trans Power Syst*. 2007;22(1):442-448.
21. Yin J, Chang L, Diduch C. A new hybrid anti-islanding algorithm in grid connected three-phase inverter system. In2006 IEEE Power Electronics Specialists Conference 2006 Jun 18 (pp. 1-7).

22. Mahat P, Chen Z, Bak-Jensen B. A hybrid islanding detection technique using average rate of voltage change and real power shift. *IEEE Transactions on Power Delivery*. 2009;24(2):764-771.
23. Vahedi H, Noroozian R, Jalilvand A, Gharehpetian GB. Hybrid SFS and Qf islanding detection method for inverter-based DG. InPower and energy (PECon), 2010 IEEE international conference on 2010 Nov 29 (pp. 672-676). IEEE.
24. Khodaparastan M, Vahedi H, Khazaeli F, Oraee H. A novel hybrid islanding detection method for inverter-based DGs using SFS and ROCOF. *IEEE Transactions on Power Delivery*. 2017;32(5):2162-2170.
25. Zhou B, Cao C, Li C, et al. Hybrid islanding detection method based on decision tree and positive feedback for distributed generations. *IET Generation, Transmission & Distribution*. 2015;9(14):1819-1825.
26. Akhlaghi S, Sarailoo M, Akhlaghi A, Ghadimi AA. A novel hybrid approach using sms and ROCOF for islanding detection of inverter-based DGs. InPower and energy conference at Illinois (PECI), 2017 IEEE 2017 Feb 23 (pp. 1-7). IEEE.
27. El-Arroudi K, Joos G, Kamwa I, McGillis DT. Intelligent-based approach to islanding detection in distributed generation. *IEEE Transactions on Power Delivery*. 2007;22(2):828-835.
28. Samantaray SR, El-Arroudi K, Joos G, Kamwa I. A fuzzy rule-based approach for islanding detection in distributed generation. *IEEE Transactions on Power Delivery*. 2010;25(3):1427-1433.
29. Faqhruldin ON, El-Saadany EF, Zeineldin HH. Islanding detection for multi DG system using inverter based DGs. In power and energy society general meeting (PES), 2013 IEEE 2013 Jul 21 (pp. 1-5). IEEE.
30. Faqhruldin ON, El-Saadany EF, Zeineldin HH. A universal islanding detection technique for distributed generation using pattern recognition. *IEEE Transactions on Smart Grid*. 2014;5(4):1985-1992.
31. Kar S, Samantaray SR. Data-mining-based intelligent anti-islanding protection relay for distributed generations. *IET Generation, Transmission & Distribution*. 2013;8(4):629-639.
32. Kersting WH. Radial distribution test feeders. *IEEE Trans Power Syst*. 1991 Aug;6(3):975-985.
33. Gagnon R. 'Detailed model of a doubly-fed induction generator (DFIG) driven by a wind turbine', The Math Work, 2006, Jan.
34. P. Giroux, G. Sybille, Hydro-Quebec research institute (IREQ), and C. Osorio, S. Chandrachood, The Mathworks, "100-kW grid-connected PV Array demo detailed model," math works file Exchange, 2012.
35. Gagnon R. 'Wind farm—synchronous generator and full scale converter (type 4) detailed model', The MathWork, 2006, Jan.
36. Std UL. 1741. Inverters, converters, and controllers for use in independent power systems.
37. Raza S, Mokhlis H, Arof H, Laghari JA, Mohamad H. A sensitivity analysis of different power system parameters on islanding detection. *IEEE Transactions on Sustainable Energy*. 2016;7(2):461-470.
38. Xue B, Zhang M, Browne WN, Yao X. A survey on evolutionary computation approaches to feature selection. *IEEE Transactions on Evolutionary Computation*. 2016;20(4):606-626.
39. Guyon I, Elisseeff A. An introduction to variable and feature selection. *Journal of Machine Learning Research*. 2003;3(Mar):1157-1182.
40. Ali M, Siarry P, Pant M. An efficient differential evolution based algorithm for solving multi-objective optimization problems. *European Journal of Operational Research*. 2012;217(2):404-416.
41. Tang J, Deng C, Huang GB. Extreme learning machine for multilayer perceptron. *IEEE Transactions on Neural Networks and Learning Systems*. 2016 Apr;27(4):809-821.
42. Akusok A, Björk KM, Miche Y, Lendasse A. High-performance extreme learning machines: A complete toolbox for big data applications. *IEEE Access*. 2015;3:1011-1025.
43. Storn R, Price K. Differential evolution—a simple and efficient heuristic for global optimization over continuous spaces. *Journal of Global Optimization*. 1997;11(4):341-359.
44. Xue B, Zhang M, Browne WN. Particle swarm optimization for feature selection in classification: A multi-objective approach. *IEEE Transactions on Cybernetics*. 2013;43(6):1656-1671.
45. Deb K, Pratap A, Agarwal S, Meyarivan TA. A fast and elitist multi objective genetic algorithm: NSGA-II. *IEEE Transactions on Evolutionary Computation*. 2002;6(2):182-197.
46. Zhai MY, Yu RH, Zhang SF, Zhai JH. Feature selection based on extreme learning machine. In machine learning and cybernetics (ICMLC), 2012 international conference on 2012 Jul 15 (Vol. 1, pp. 157-162). IEEE
47. Huang GB, Zhou H, Ding X, Zhang R. Extreme learning machine for regression and multiclass classification. *IEEE Trans Syst Man Cybern B Cybern*. 2012;42(2):513-529.

How to cite this article: Chandak S, Mishra M, Rout PK. Hybrid islanding detection with optimum feature selection and minimum NDZ. *Int Trans Electr Energ Syst*. 2018;28:e2602. https://doi.org/10.1002/etep.2602